DOI: 10.21776/ub.jpacr.2017.006.03.345 *J. Pure App. Chem. Res.*, **2017**, 6(3), 207-220
3 September 2017

The Effect of Phosphatation and Granulation Zeolite in the Adsorption of Cr(VI)

Sri Wardhani*, Danar Purwonugroho, Reno Sunarinda Endrayana

Department of Chemistry, Faculty of Mathematics and Natural Sciences, Brawijaya University

*Corresponding email : Wardhani.ub@gmail.com
Email author 1: danar@ub.ac.id
Email author 2: renosunarindaendrayana@gmail.com

Received 6 July 2017; Revised 5 August 2017; Accepted 21 August 2017

ABSTRACT

This research was aimed to study the effect of contact time on adsorption of Cr(VI) using Granules Alumino Silico Phosphate (GASP) and to determine the adsorption capacity of GASP. The GASP synthesis process was carried out in several main stages: 1) activation of zeolite with addition 0.4 M HCl, 2) Zeolite phosphatation by addition of $NH_4H_2PO_4$ ratio Si/P = 1/6 at 235^{O}C for 5 hours, 3) Granulation of phosphated zeolite using chitosan to afford the GASP. The GASP was characterized using XRF, FT-IR and SAA. The contact time effects was tested using 0.1 g of GASP in K_2CrO_4 100 mg/L and the contact time variation of 0.5; 1.0; 1.5; 2.0 and 2.5 hours. The result of the research showed that the optimum contact time occurred for 2 hours. The concentration effect on adsorption capacity was tested out using 0.1 g of GASP in K_2CrO_4 and the concentration variation of 25, 50, 75, 100 and 150 mg/L for 2 hours. The adsorption capacity can be determined using the Langmuir equation. XRF characterization results showed an emergence of P_2O_5 34.70 % and decrease in SiO_2 levels of 18.10% and Al_2O_3 by 2.2% after phosphatation process. The result of characterization by FTIR indicated the success of the phosphatation process as evidenced by the shift of wavenumber to the lower region of tetrahedral silica and alumina uptake was shifted to wavenumber the region of tetrahedral phosphate uptake in accordance with Hooke's law. Characterization results by SAA showed increased surface area, pore volume and pore count after phosphatation process. The concentration variation was directly proportional to the increase of the adsorbed Cr(VI) mass. The presence of phosphatation and granulation process can increase the value of adsorption capacity by 48.077 mg/g on GASP rather than 15.601 mg/g on active zeolite

Key words: adsorption capacity, ASP, concentration, contact time, Cr(VI), granulation, phosphatation

INTRODUCTION

Nowadays, tannery industry still generates a lot of liquid waste discharged into the aquatic environment. The liquid waste contains a chromium (Cr) compound in the form of chromium sulfate ($Cr_2(SO_4)_3$). High levels of $Cr_2(SO_4)_3$ of 60-70% is not entirely absorbed by the skin during the tanning process, the solution is removed to the environment as hazardous and toxic substances.[1]. Besides that, Cr (III) in the wastes can be oxidized to produce Cr(VI) which has high toxicity with content of Cr(VI) in the waste of 0.2 - 218.5 mg/L. Cr(VI) has several disadvantaged impacts in the human, such as skin irritation, systemic poisoning (damage to internal organs) and incidence of cancer in long period when it accumulated in the body. According to the United Nationals Industrial Development

The journal homepage www.jpacr.ub.ac.id
p-ISSN : 2302 – 4690 | e-ISSN : 2541 – 0733

Organization (UNIDO) on the liquid waste quality standard for industrial activities in 2000, the maximum limit of Cr(VI) in water was 0.1 - 0.5 mg/L[2].

The Cr(VI) formed in the waste need to be adopted to reduce their toxicity by using an adsorbent such as zeolite. Zeolite is a mineral aluminosilicate hydrate which has a unique structure that is the presence of alumina groups (AlO_4^-) and silica groups (SiO_4) interconnected by oxygen atoms form a three-dimensional framework. Zeolite also has a porous crystal structure, and has a large surface area. Beside as the zeolite adsorbent it can also applied as a catalyst, molecular filter and ion exchange[3]. The zeolite adsorption capability is not only influenced by pore size but also the positive and negative charges contained in the pores of the zeolite. The charge is capable of binding negative and positive molecular ions by involving electrostatic forces (chemical adsorption)[4].

Natural zeolites generally have relatively low both pore size and positive charges. Both can be improved by activation using strong acid and modification of zeolite by ammonium dihydrogen phosphate ($NH_4H_2PO_4$) through phosphatation process. In the phosphatation process of neutral (SiO_4) or negative charge (AlO_4^-) in the zeolite will be replaced by positive charged (PO_4^+). Increasing of the positive charge on zeolite may improve its Cr(VI) adsorption capacity [5]. According to [6–8] the optimum phosphatation process occurs at a temperature of 235^oC was using ammonium dihydrogen phosphate ($NH_4H_2PO_4$) for 5 hours because under such conditions $NH_4H_2PO_4$ would decompose free ammonia. Therefore, there is no NH_4^+ ions can interfere with the phosphatation process.

According to Suraya [9], at the optimum pH 4 to 0.1 g of Alumino Silico Phosphate (ASP) Si/P ratio of 1:6 (mol/mol) was obtained by adsorption percentage of 29.53%. So it is necessary to do research the influence of contact time and adsorption capacity of Alumino Silico Phosphat (ASP) in the form of granule. The addition of chitosan to Granules Alumino Silicon Phosphate (GASP) not only used as adhesive but also can increase the adsorption capacity of Cr(VI) due to the presence of amine groups ($-NH_3^+$) in zeolite. This can be proved based on the results of the study[10] which reported the adsorption capacity of chitosan zeolite granules of 4.05 mg/g greater than the zeolite powder adsorption capacity of 3.48 mg/g against anionic waste (phosphate ions). In addition, ASP in the form of granules can easily be separated from the adsorbate process compared to the form of powder. This research will investigate about the effect of phosphatation and granulation zeolite in the adsorption of Cr(VI). The zeolite utilized a natural zeolite from the Blitar city.

EXPERIMENT

Materials and instruments

Materials used in this research include zeolite, HCl (Merck), distilled water, ammonium dihydrogen phosphate (SAP), ammonium molybdate (Merck), nitric acid (Merck), chitosan (Merck), glacial acetic acid (Merck), Sodium Hydroxide (Merck), Potassium Chromate (Merck), and 1,5-diphenylcarbazid (Merck).

The instruments used in this study are magnetic stirer, UV-Vis spectrophotometer (Shimazu), analytical balance, furnace 6000 (Barnstead Thermolgne), oven (Memmert), sieve of 150 mesh and 200 mesh, syringe pump type BYZ-810T Byond), shaker (Wise Shake), hot plate, Fourier Transformation Infrared (FT-IR) 8400S, X-Ray Fluorescence (XRF) Minipal 4 type (PANalytical), Surface Area Analyzer (SAA), Porcelain cup and glassware.

Procedure of zeolite activation

A fine zeolite was obtained by using a sieve size between 150 mesh and 200 mesh. Before activation process, 20 g zeolite was washed with 250 mL of distilled water and stirred

with a magnetic stirrer for 1 hour. Then zeolite was filtered and dried at 105^{O}C. A dried zeolite was mixed with 0.4 M HCl with a ratio of 1 g zeolite / 10 mL HCl for 4 hours stirred with a magnetic stirrer. Active zeolite was rinsed with distilled water to pH filtrate 7 then dried at 105^{O}C.

Procedure of phosphatation zeolite

An active zeolite of 6 g was mixed with 45.552 g ammonium dihydrogen phosphate (ratio of Si/P: 1/6). The mixture was heated at 235^{O}C for 5 hours. Then settled at room temperature and washed by distilled water until the filtrate was free of phosphate ions. Qualitative test of phosphate ions to added a solution of $Mg(NO_3)_2$ (formed white precipitate)[11]. The residue was dried at 105^{O}C to obtain Alumino Silico Phosphate (ASP) powder. ASP was characterized using X-Ray Fluorescence (XRF).

Procedure of Granules Alumino Silico Phosphate (GASP) manufacturing

ASP of 3 g was mixed with 0.18 g of chitosan and 9 mL of 2% acetic acid, then stirred by magnetic stirrer until homogeneous. ASP-chitosan was dripped into 1 M NaOH solution used syringe pump until granules was formed. Then granules was washed with distilled water until pH filtrate reaches 7 and dried at 105^{O}C to obtain Granules Alumino Silico Phosphate (GASP). GASP was characterized using Fourier Transformation Infrared (FT-IR). As a comparison, granules preparation was also performed for active zeolite.

Procedure for determining the optimal contact time GASP on Cr(VI) adsorption

GASP of 0.5 g was added 25 mL of K_2CrO_4 100 mg/L into 250 mL erlenmeyer flasks on pH 6.3 – 7.1 and shuffled with shaker at 100 rpm. Used variations of contact time 0.5; 1.0; 1.5; 2.0 and 2.5 hours. The mixture was separated between the filtrate and the adsorbent through the filtration process. The filtrate was taken and the determination of Cr (VI) content with complexing of 1.5-diphenylcarbazide acidic condition pH ≤ 2(acetic acid)[11]. Then the filtrate was measured using a spectrophotometer UV-Vis at a wavelength of 541 nm.

Procedure for determination the effect of Cr (VI) concentration on adsorption capacity at GASP

A 25 mL of K_2CrO_4 solution 25, 50, 75, 100 and 150 mg/L were added adsorbent 0.1 g GASP in erlenmeyer flasks and shuffled by shaker at 100 rpm in optimum contact time. The filtrate was taken and the determination of Cr(VI) content and complex of 1.5-diphenylcarbazide in acidic condition (acetic acid). Then the filtrate was measured using a spectrophotometer UV-Vis at a wavelength of 541 nm. As a comparison, the adsorption capacity was also performed on the active zeolite, active zeolite granule and ASP powder.

RESULT AND DISCUSSION

X-Ray Fluorescence (XRF)

The analysis using XRF has been conducted to identify composition in active zeolite, ASP and GASP. XRF spectra of active zeolite and Alumino Silico Phosphate (ASP) are shown in **Figure 1** and **Figure 2**. While the interpretation of the XRF spectra of active zeolite and Alumino Silico Phosphate (ASP) shown in **Figure 3**.

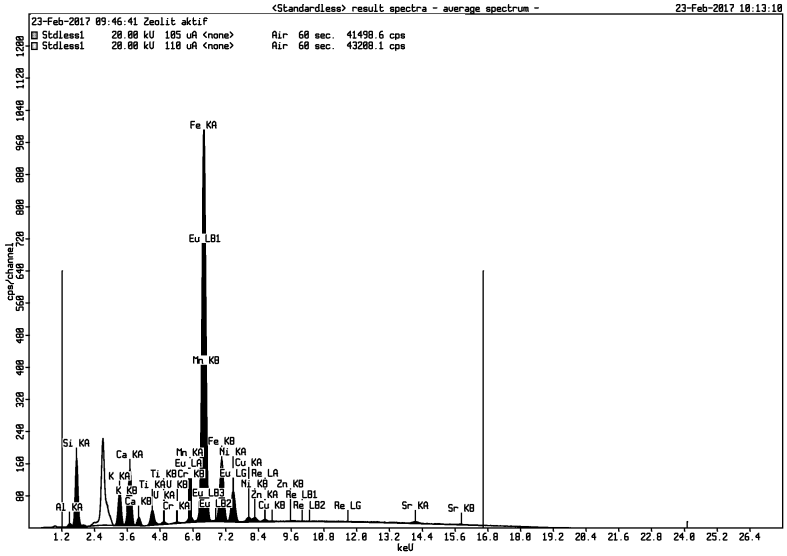

Figure 1. Active zeolite XRF spectra.

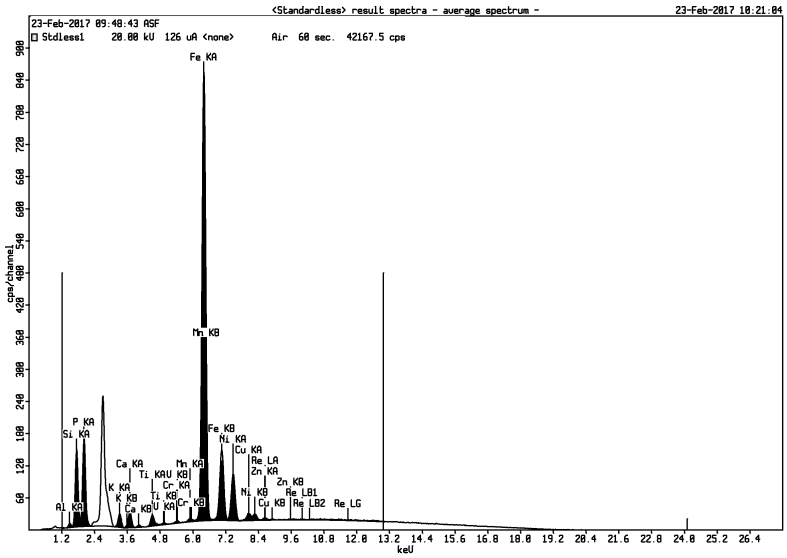

Figure 2. ASP XRF spectra.

In the XRF data of active zeolite **Figure 1** and **Figure 3** the content of silica (SiO_2) and alumina (Al_2O_3) based on the zeolite framework is 64.30 % (wt) and 8.30 % (wt). From the silica content can be predicted the $NH_4H_2PO_4$ mass required in the zeolite phosphate process with the Si/P ratio: 1/6 (mol/mol). Although the zeolite has been activated, there are still high impurity compounds such as Fe_2O_3 14.70 % (wt), CaO 5.51 % (wt) and K_2O 3.65 % (wt).

The content of silica (SiO_2) and alumina (Al_2O_3) in **Figure 3** decreased after phosphatation process from 46.20 % (wt) and 6.10 % (wt) along with the emergence of P_2O_5 oxide from $NH_4H_2PO_4$ addition of 34,70 % (wt). In addition, the impurities of Fe_2O_3, CaO and K_2O also decreased to 9.26 % (wt), 0.97 % (wt) and 1.00 % (wt). The emergence of the P_2O_5 oxide compound may be connected to the isomorphic substitution of the zeolite framework during the phosphatation process and/or free phosphate ions without isomorphic substitution.

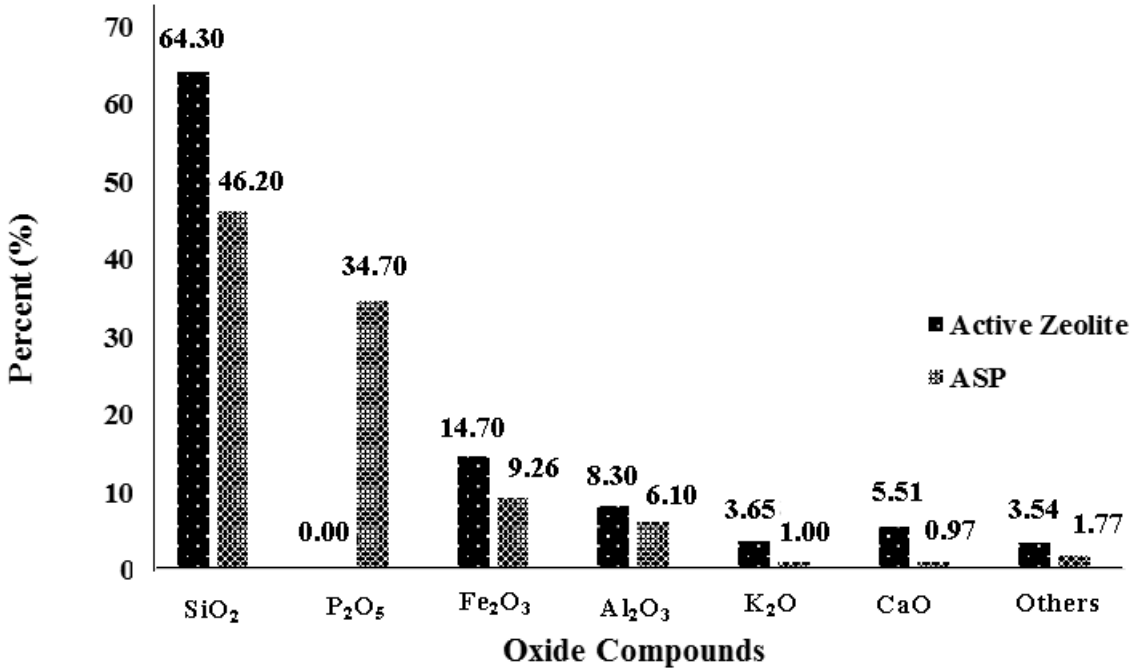

Figure 3. Relationship of percent (%) to the types of oxide compounds.

Compared to the alumina groups, silica groups tend to be easily replaced by phosphate groups because of some similarities in their properties. As the same length of Si-O bonds in silica is 1.63 Å and P-O in phosphate of 1.63 Å compared to Al-O in alumina of 1.75 Å. The amount of bond length on alumina causes stability also increases. In addition, the Al-O binding energy of alumina is 512 kJ/mol greater than the bonding force of Si-O in silica of 452 kJ/mol and P-O in phosphate of 335 kJ/mol [12,13]. Therefore, alumina is more difficult accomplished phosphatation than silica. The success of zeolite phosphatation in detail can be determined by characterization with FTIR and the adsorption results of phosphate adsorbent (ASP and GASP).

Fourier Transform Infrared Spectroscopy (FT-IR)

The analysis using FTIR aimed to determine the functional groups contained in active zeolites, ASP and GASP. The IR spectra pattern of active zeolite, Alumino Silico Phosphate (ASP) and Granules Alumino Silico Phosphate (GASP) are shown in **Figure 4** and the interpretation of the IR spectra pattern represented in **Table 1**.

Based on **Figure 4** and **Table 1** of numbers 1, O-H stretching on active zeolite and GASP indicates the presence of H_2O entering in the pores of the zeolite. The presence of amplified H_2O in numbers 5 appears to bend O-H from active zeolite, ASP and GASP. The O-H group on ASP did not appear in numbers 1 due to a little content of H_2O caused the intensity appears too low and not strong adequately to produce the peak. The evidence of chitosan during the manufacturing of Granules Alumino Silico Phosphate (GASP) can be known in numbers 3 of C-H asymmetric stretching from GASP. This result was also ensured in number 1 that O-H stretching of chitosan, number 2 N-H asymmetry stretching and number 4 N-H symmetric stretching of chitosan.

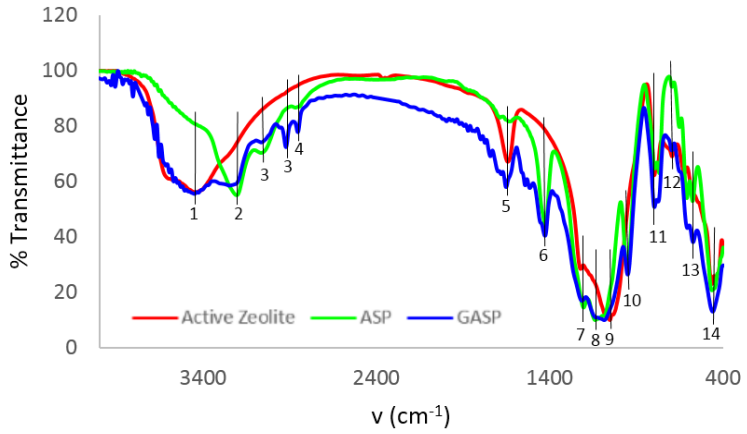

Figure 4. Infra-red spectra of active zeolite, ASP and GASP.

Table 1 Interpretation of infrared spectra on active zeolite, ASP and GASP

Numbers	Active zeolite	ASP	GASP	Absorption
1	3443.46	-	3449.25	O-H stretching (H_2O and chitosan)[14]–[16]
2	-	3206.23	3246.74	N-H asymmetry stretching ($NH_4H_2PO_4$ and chitosan)[17]
3	-	-	3063.51 2920.79	C-H asymmetric stretching (chitosan)[14], [16]
4	-	2866.79	2853.29	N-H symmetric stretching ($NH_4H_2PO_4$ and chitosan)[14]
5	1642.07	1686.43 1638.21	1651.72	O-H bending (H_2O) [14]
6	-	1426.06	1427.99	P=O bending [17], [18]
7	1223.55	1206.19	1213.90	Asymmetric external linkage stretching (O-Si-O and O-Al-O)[19]
8	-	1138.69	1130.97	PO_4 stretching (O-P-O) [17], [18]
9	1053.82	1086.61	1086.61	Asymmetric internal tetrahedral stretching (O-Si-O and O-Al-O)[16], [20]
10	-	953.53	951.6	PO_4 stretching (O-P-O)[17], [18]
11	797.31 779.95	795.38 768.38	797.31	Symmetric external linkage stretching (O-Si-O and O-Al-O)[19], [20]
12	695.09	695.09 652.66	697.02	Symmetric internal tetrahedral stretching (O-Si-O and O-Al-O)[20]
13	-	577.44	573.58	Tetrahedral PO_4 (O-P-O, O=P-O)[15]
14	465.58	465.58	459.79	Tetrahedral bending (Si-O-Si and Al-O-Al)[16], [20]

Numbers 2 and 4 also showed the presence of an N-H group of NH_4^+ from $NH_4H_2PO_4$ reactants attached to the zeolite framework. The results showed that not all NH_4^+ turns into NH_3 gas during phosphatation process. Numbers 6, 8, 10 and 13 respectively show P=O bending, PO_4 stretching (O-P-O), PO_4^- stretching (O-P-O) and tetrahedral PO_4 was occurred on ASP and GASP adsorbents. This proves the occurrence of isomorphic substitution between alumina (AlO_4^-) and silica (SiO_4) groups with phosphate (PO_4^+) during the phosphatation process. In addition, the isomorphic substitution caused a shift toward the lower wavenumber. Number 7, 9 and 12 including the asymmetric external linkage stretching

TO_4 (O-Si-O and O-Al-O), asymmetric internal tetrahedral stretching (O-Si-O and O-Al-O) and symmetric internal tetrahedral stretching (O-Si-O and O-Al-O) of the active zeolite which shifts into numbers 8, 10 and 13 of the ASP and GASP. Based on the Hooke's law, increasing of atom mass from Si-O (Mr: 42.98 g/mol) and Al-O (Mr: 44.084 g / mol) to P-O (Mr: 46.972 g/mol) caused shifting of wavenumbers to a lower one[19]. Despite the shifts, on numbers 7, 9 and 12 of the ASP and GASP adsorbents still produce peaks indicating that was not all alumina (AlO_4^-) and silica (SiO_4) groups are replaced by phosphate groups (PO_4^+).

Surface Area Analyzer (SAA)

Analysis by using SAA to determine surface area, pore volume and average pore radius or pore distribution on granules active zeolite and GASP. The results of SAA characterization were presented in **Figure 5**, **Figure 6** and **Figure 7**.

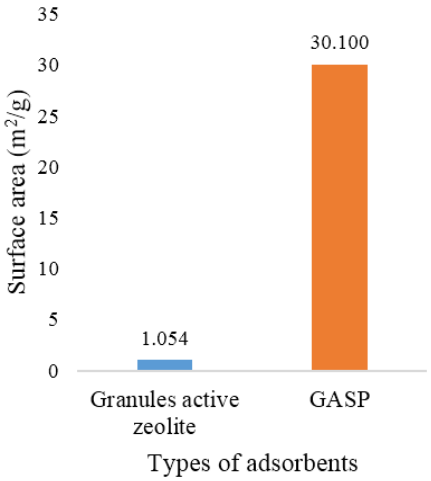

Figure 5. Surface area data (m^2/g) on granules active zeolite and GASP

Based on **Figure 5** on GASP has a surface area 30.100 m^2/g larger than granules active zeolite 1.054 m^2/g. In **Figure 6** GASP also has a pore volume of 1.262 cm^3/g greater than the granules active zeolite of 0.354 cm^3/g. This suggested that the phosphate process not only improves the positive sites but also can increase the surface area and pore volume of the zeolite. In addition, in **Figure 7** the average pore radius of GASP is 838.6 Å lower than the granules active zeolite of 6714 Å. This indicated that increased surface area and pore volume after the phosphatation process cause the decrease of average pore radius. The average pore radius showed how close the inter-pore distance is in the adsorbent. Therefore, by lowering average pore, the radius pores was closer and afforded more pores on the adsorbent.

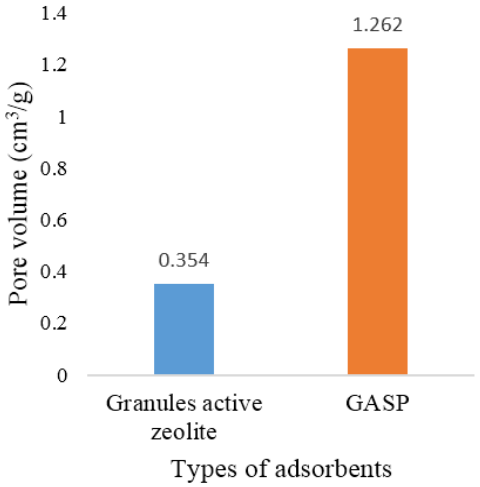

Figure 6. Pore volume data (cm^3/g) on granules active zeolite and GASP

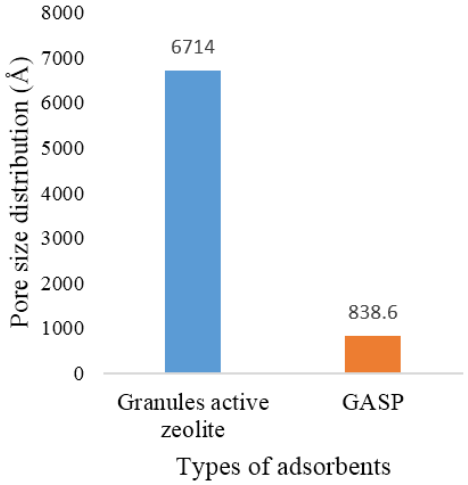

Figure 7. Pore size distribution data (Å) on active zeolite granules and GASP

Effect of optimum contact time GASP on Cr(VI) adsorption

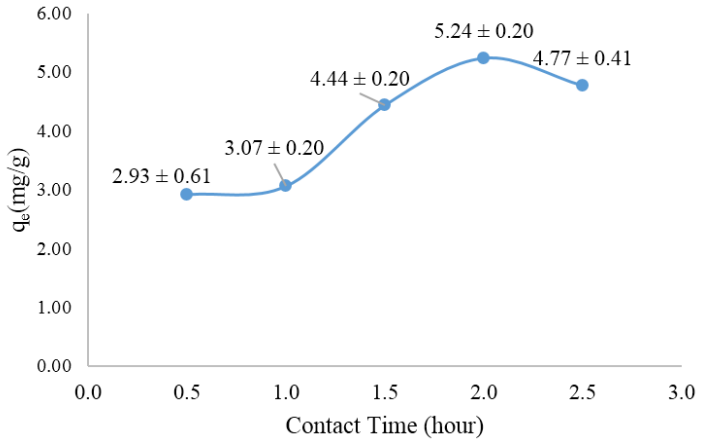

Figure 8. The relation of adsorption contact time (hour) to Cr(VI) mass which absorbed per gram of GASP adsorbent (q_e).

Figure 8 shows that the optimum time of the adsorption process occurs at 2 hours with Cr(VI) ion mass absorbed per gram of adsorbent (qe) of 5.24 ± 0.20 mg/g. Adsorption of Cr(VI) increased from 0.5 to 2 h probably due to active sites and surface area of GASP. While at contact time from 2 hours to 2.5 hours, qe the adsorption decreased from 5.24 ± 0.05 mg / g to 4.77 ± 0.10 mg/g. This occurs because positive sites/ active sides of the GASP adsorbent may be fully charged by Cr(VI) so that the adsorbent is saturated and causes desorption / release of Cr(VI) from the adsorbent back to the adsorbate. According to the result of research Mutngimaturrohmah and Khabibi [20] that at certain times the mass of Cr(VI) will increase and then decrease after the Cr(VI) concentration has equilibrium in the adsorbent and adsorbate.

Effect of Cr(VI) concentration on adsorption capacity in GASP

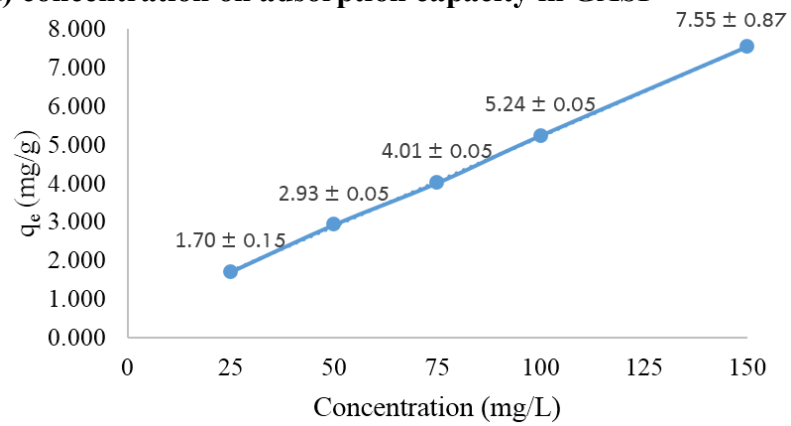

Figure 9. The relation of Cr(VI) concentration to Cr(VI) mass which absorbed per gram of GASP adsorbent (q_e)

Figure 9 showed that the increased concentration of Cr(VI) results in the mass of Cr(VI) adsorbed by GASP also increases. Cr(VI) mass absorbed per gram of adsorbent (qe) continues to increase from concentrations of 25 mg/L to 150 mg/L respectively 1.70 ± 0.15; 2.93 ± 0.05; 4.01 ± 0.05; 5.24 ± 0.05 and 7.55 ± 0.87 mg/g. This occurred because the GASP adsorbent has large pores and positive sites / active sides. Therefore, the increase of Cr(VI) mass was required to fully occupy all of the active side until it becomes saturated. Based on the theory, the increased concentration of adsorbate, the amount of soluble that can be adsorbed until the equilibrium condition was also increases. The equilibrium condition occurred when the rate of the absorbed substance is equal to the rate of the substance released from the adsorbent at a certain temperature[21].

Based on the data as shown in **Figure 9,** the maximum adsorption capacity of the GASP adsorbent was determined by the Langmuir equation. The Langmuir equation (equation 1) assumed that the maximum adsorption capacity occurred in a single layer (monolayer) adsorbate on the surface of the adsorbent[21,22]. The graph was depicted in **Figure 10**.

$$\frac{C_e}{q_e} = \frac{1}{q_m b} + \frac{1}{q_m} C_e$$

C_e = Concentration of adsorbate ion in solution after adsorption (mg/L)
q_e = The adsorbate ion mass absorbed per gram of adsorbent (mg/g)
b = Langmuir constant / affinity parameter (L/mg)

q_m = Maximum adsorption capacity (mg/g)

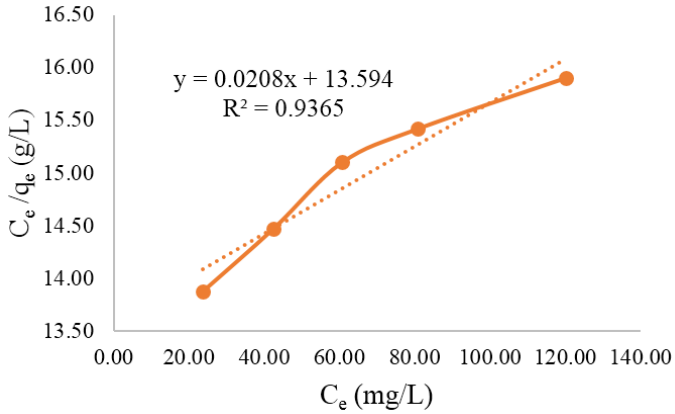

Figure 10. Langmuir equations on GASP from Cr(VI) concentration after adsorption process (C_e) to concentration per Cr(VI) mass which absorbed per gram of adsorbent (C_e/q_e).

In **Figure 10** the coefficient of determination $R^2 \geq 0.9$ (close to 1.0) showed that the equation y= 0.0208x +13.594 satisfies the Langmuir Equation with R^2 = 0.937. Based on slope value ($1/q_m$) = 0.0208, maximum adsorption capacity(q_m) on GASP adsorbent can be determined that is 48,077 mg/g. Maximum adsorption capacity is also determined for active zeolite, granules active zeolite and Alumino Silicone Phosphate (ASP), respectively **Figure 11**, **Figure 12** and **Figure 13**.

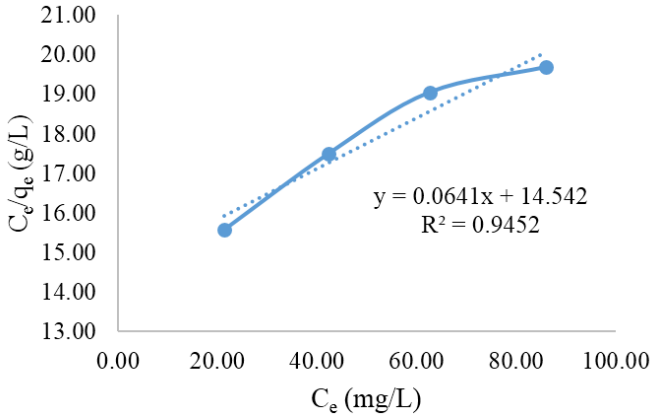

Figure 11. Langmuir equations on active zeolite from Cr(VI) concentration after adsorption process (C_e) to concentration per Cr(VI) mass which absorbed per gram of adsorbent (C_e/q_e).

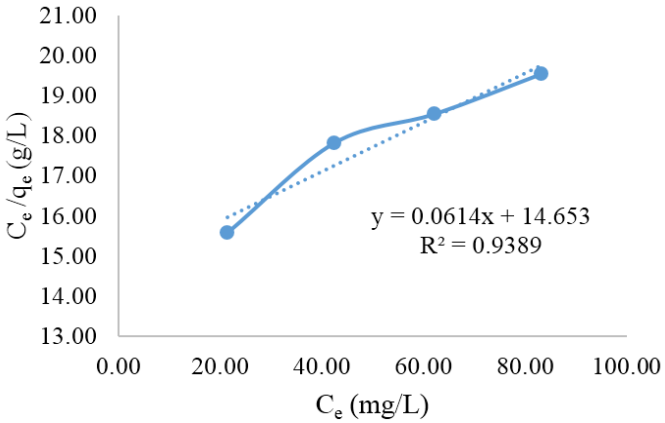

Figure 12. Langmuir equations on granules active zeolite from Cr(VI) concentration after adsorption process (C_e) to concentration per Cr(VI) mass which absorbed per gram of adsorbent (C_e/q_e).

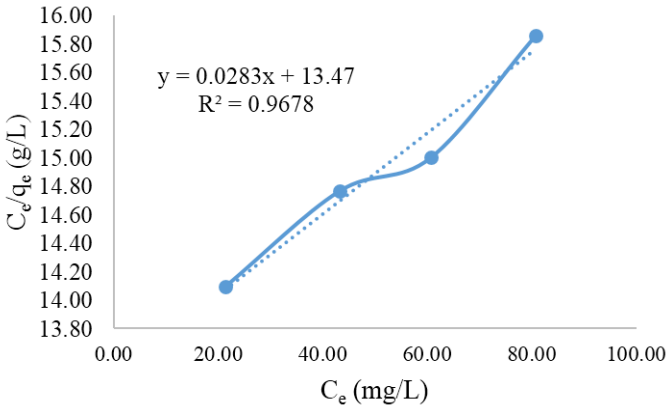

Figure 13. Langmuir equations on ASP from Cr(VI) concentration after adsorption process (C_e) to concentration per Cr(VI) mass were absorbed per gram of adsorbent (C_e/q_e).

The coefficient of determination (R^2) employed to investigate the effect of magnitude (x) on the dependent variable (y), if the value is close to 1.0 then the langmuir equation can be used. The coefficient of determination (R^2) on the active zeolite, active zeolite granules and ASP has $R^2 \geq 0.9$ (close to 1.0) to satisfy the Langmuir equation with R^2 value of 0.945; 0.939 and 0.968. The maximum adsorption capacity could be determined by using the slope value of each equation on the active zeolite, granules active zeolite and ASP [21], [22]. Then difference of adsorption ability based on maximum adsorption capacity value on each of the adsorbent as in **Figure 14.**

Figure 14 showed that GASP (48.077 mg/g) is the highest maximum adsorption capacity in other types of adsorbents (active zeolite, granules active zeolite and ASP). This occurs because the ASP adsorbent has a large positive sites/ active sides of the phosphatation zeolite phosphate with ammonium dihydrogen phosphate and addition of chitosan so as to adsorb more anions / Cr(VI). Positive sites/ active sides is PO_4^+ on the phosphatation zeolite layer and the $-NH_3^+$ functional group of chitosan. In addition, increased surface area, pore volume and pore amount (the result of SAA characterization) may also serve as a factor in increasing maximum adsorption capacity in GASP. The effect of a phosphatation zeolite can also be known from the maximum ASP adsorption capacity of 35.336 mg/g which is greater than the active zeolite of 15.601 mg/g. This is consistent with the theory that in the phosphate

process of neutral or negatively charged AlO_4^- charged SiO_4 structures in the zeolite will be replaced by a positive charged PO_4^+ structure which causes positive charge increase so that the maximum adsorption capacity also increases[5]. The reaction of functional group substitution in isomorph substitution is in **Figure 15**.

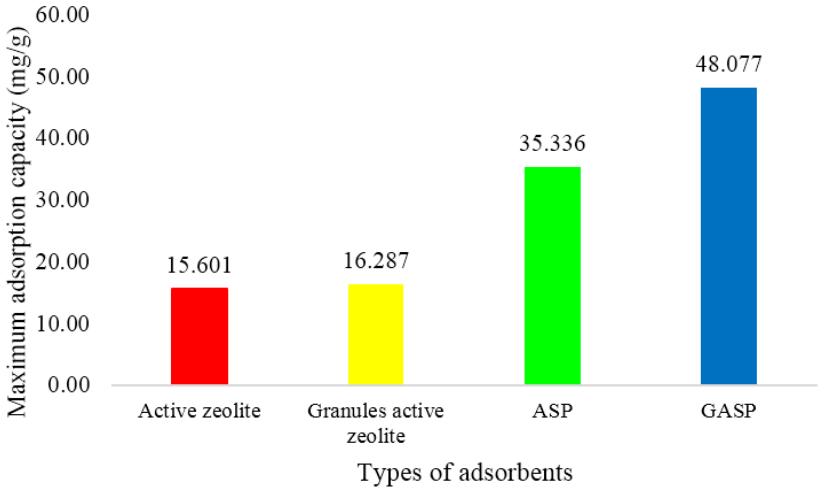

Figure 14. Maximum adsorption capacity on different adsorbents.

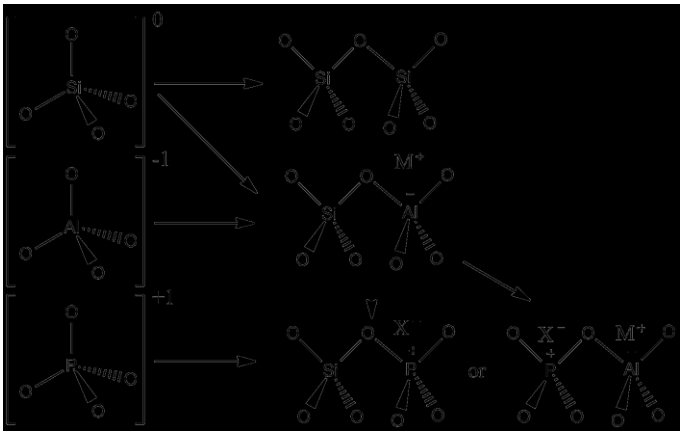

Figure 15 Isomorphic substitution reactions[5]

Meanwhile, the effect of chitosan addition can be investigated by the value of maximum adsorption capacity between active zeolite and granules active zeolite and ASP with GASP. The presence of chitosan on the granules active zeolite causes the maximum adsorption capacity of granules active zeolite 16.287 mg/g greater than active zeolite that is 15.601 mg/g. Similarly, GASP has a maximum adsorption capacity of 48.077 mg/g greater than ASP of 35.336 mg/g. In addition, to functioning as an adhesive, the addition of chitosan into the zeolite can increase the adsorption capacity of Cr(VI) in pH adsorption 7.0 - 6.3 because chitosan is able to form crosslinks with zeolite and has an amine group ($-NH_3^+$) capable of binding Cr(VI) in pH ≤ 6,5[23], [24].

The existence of large difference of distance at value of adsorption capacity between active zeolite to active zeolite granule from 15.601 mg/g to 16.287 mg/g with ASP to GASP that is from 35.335 mg/g to 48.077 mg/g caused by ammonium ion (NH_4^+) in ASP (evidenced from the uptake of ammonium ions in IR spectra). When chitosan was added to

ASP, the pH of the solution is about 6.5 at the time of adsorption which is the amine group (-NH_2) in chitosan undergoes a protonation producing a positively charged amine group (-NH_3^+). The increasing number of positively charged amine groups (-NH_3^+) in chitosan is directly proportional to the increased adsorption capacity of Cr(VI) and can increase the distance of the adsorption capacity difference between ASP and GASP.

CONCLUSION

The result of XRF characterization results showed an emergence of P_2O_5 34.70 % and decrease in SiO_2 levels of 18.10% and Al_2O_3 by 2.2% after phosphatation process. The phosphate process was successfully conducted which evidenced by the shift of wave numbers to the lower region at wave number of tetrahedral silica and alumina uptake shifted to wavenumber of tetrahedral phosphate uptake in accordance with Hooke's law. Characterization results with SAA showed increased surface area, pore volume and pore count after phosphatation process. The variation of contact time influences the increasing of Cr(VI) adsorption. The optimum contact time occurs in the adsorption process for 2 hours. The concentration variation is directly proportional to the increase of the adsorbed Cr(VI) mass. The presence of phosphatation and chitosan addition process can increase the value of adsorption capacity by 48.077 mg/g in GASP compared without phosphate process and chitosan addition of 15.01 mg/g in active zeolite.

REFERENCES

[1] Suwarno, H. and Tandjung, S. D., *J. Teknosains*, **2014**, 3(2), 132–141.
[2] Bosnic, M., Buljan, J. and Daniels, R.P., *Pollutants in Tannery Effluent: Limits for Discharge into Water Bodies and Sewers,* United Nations Industrial Development Organization (UNIDO) , **2000**, US/RAS/92/120, pp. 1–26.
[3] Lemoine, G. *Comparison of Different Types of Zeolites Used As Solid Acid Catalysis in The Transesterificatin Reaction of Jatropha-type Oil for Biodiesel Production*, M.Sc. Thesis, Worcester Polytechnic Institute, **2013,** pp. 75-80.
[4] Wirawan, S. K., Sudibyo, H. and Setiaji, M. F., *JESTEC*, **2015,** 3, 87–95.
[5] H Faghihian, MH Mohammadi, *Iran J Chem Chem Eng*, **2008**, 27(4), 115–118.
[6] Elok, K. H., Study of Effect of Phosphate Compound on Natural Zeolite Phosphate, Faculty of Mathematics and Natural Sciences, Brawijaya University, Malang, **2002**.
[7] Agustina, E., Study of the Effect of Temperature of Phosphate on the Zeolite Turen Anion Natural Exchange, Faculty of Mathematics and Natural Sciences, Brawijaya University, Malang, **2002**.
[8] Praswanto, S. A., Study of the Effect of Mol Si / P Comparisons on Zeolite Nature Turen Phosphatation, Faculty of Mathematics and Natural Sciences, Brawijaya University, Malang, **2001**.
[9] Suraya, Z., Variation of pH of Solution and Adsorbat Concentration on Anion Adsorption Formed Cr (VI) by Zeolite Result of Phosphate, Faculty of Mathematics and Natural Sciences, Brawijaya University, Malang, **2003**.
[10] Xie, J., Li, C., Chi, L. and Wu, D., *Fuel*, **2013**, 103, 480–485.
[11] Vogel, Textbook Qualitative Inorganic Analysis Macro and Semimicro, Fifth Edition, **1990**, PT. Kalman Media Pusaka, Jakarta.
[12] Huheey, P., The Strengths of Chemical Bonds, 2nd Edition, **1958**, Butterworths, London.
[13] Stuck, J. W. and Banwart, W. L., *Advanced Chemical Methods for Soil and Clay Mineral Research*, **1979**, D. Reidel Publishing Company, Illinois, USA.

[14] Silva, S. M. L., Braga, C. R. C., Fook, M. V. L., Raposo, C. M. O., Carvalho, L. H. and Canedo, E. L., *Mater. Sci. Eng. Technol.*, **2011**.
[15] Jegatheesan, A., Murugan, J., Neelakantaprasad, B. and Rajarajan, G., *Int. J. Comput. Appl.*, **2012,** 53, 4, 53–56.
[16] Utubira, Y. and Al, E., *Indo J .Chem*, **2006**, 6, 231–237.
[17] Nirmala, B., Sudha, A. G. and Suresh, E., *Soc. Educ.*, **2013**, 4, 45–51.
[18] Ahsan, M. R., Uddin, M. A. and Mortuza, M. G., *IJPAP*, **2005**, 43, 89–99.
[19] Jannah, M., Armilasari, N. and Prasetyoko, D., *J. Sains and Art Pomits*, **2014**, 2(1), 1–9.
[20] Mutngimaturrohmah, Gunawan, and Khabibi, *J. Clays dan Clays*, 2009, 1–7.
[21] Kalsi, P. S., Spectroscopy of Organic Compounds, Sixth Edit, **2004**, New Age International (P) Ltd., New Delhi.
[22] Emelda, L., Putri, S. M., and Ginting, S*., J. Chemical And Environment Engineering*, **2013**, 9, 166–172.
[23] Handayani, M. and Sulistiyono, E., *Langmuir and Freundlich Equation Test on Chrom Waste Absorption (VI) by Zeolite*, *Pros. Semin. Nas. Sains dan Teknol. Nukl. PTNBR Bandung*, **2009**, pp. 130–136.
[24] Liu, Y. and Chen, J., Ionic Liquids for Better Separation Processes, **2016**, Springer, Berlin.
[25] De Alvarenga, E. S., *Characterization and Properties of Chitosan*, in *Biotechnology of Biopolymers*, **2011**, vol. 5, pp. 91–109.
[26] Safitri, A., Mulyasuryani, A., and Sabarudin, A., *Student J.*, **2013**, 1(1), 8–14.